RSC Advances

PAPER

View Article Online
View Journal | View Issue

Cite this: *RSC Adv.*, 2025, **15**, 30427

Enhancing lithium metal batteries with a nano-silicon nitride-based solid electrolyte interface layer

Roya Damircheli, †[a] Odalys Cristina Campos, †[b] Binh Hoang [a] and Chaun-Fu Lin*[a]

Lithium metal batteries promise high energy density but suffer from unstable solid–electrolyte interphases that promote dendrite growth and premature failure. Here we report a simple drop-casting pretreatment that deposits a uniform layer of nano-sized silicon nitride (Si_3N_4 <50 nm) onto lithium foil, forming a Li_3N-rich artificial interphase. Two loadings, 0.2 and 1 wt%, were evaluated under rinsed and non-rinsed conditions. Structural and chemical characterization results from SEM and X-ray diffraction show that the non-rinsed 1 wt% coating yields a dense, uniform layer dominated by Li_3N. Electrochemical impedance spectroscopy reveals a stable low charge-transfer resistance, and symmetric-cell cycling at 1 mA cm^{-2} demonstrates a lifespan of 1375 hours, compared with 950 hours for the rinsed sample and 280 hours for untreated lithium. The improved performance is attributed to the electrochemically stable, ionically conductive, and mechanically robust Li_3N-based interphase that suppresses dendrite formation and preserves interfacial contact. This work highlights nano-Si_3N_4 as an effective additive for enabling safer and longer-lasting high-energy lithium metal batteries.

Received 15th July 2025
Accepted 19th August 2025

DOI: 10.1039/d5ra05077d

rsc.li/rsc-advances

1 Introduction

Lithium-ion batteries (Li-ion) have transformed energy storage, serving as the backbone for portable electronics, electric vehicles, and grid-scale applications due to their high energy density and long operational lifespan.[1–4] However, the increasing demand for even greater energy capacity has driven extensive research into lithium metal batteries (LMBs) as a next-generation solution. LMBs gained significant attention due to their exceptionally high theoretical specific capacity of approximately 3860 mAh g^{-1} and low reduction potential (−3.04 V *vs.* the standard hydrogen electrode), making them a promising candidate for advancing energy storage technology.[5–8] However, despite these advantages, the practical implementation of lithium metal anodes faces considerable challenges related to safety, cycle life, and performance degradation. One of the primary obstacles hindering the commercialization of LMBs is the uncontrolled growth of lithium dendrites.[9–12] These needle-like structures form on the anode surface during electrochemical cycling due to the instability of the solid–electrolyte interphase (SEI).[13–16] The inherent inability of the SEI to accommodate the dynamic morphological and volumetric changes of lithium during repeated cycling results in dendrite proliferation, continuous electrolyte consumption, and rapid capacity fading.[17,18] More critically, lithium dendrites can penetrate the separator, causing internal short-circuits, thermal runaway, and severe safety hazards, ultimately compromising the reliability of lithium-ion batteries.[19,20]

To address these challenges, extensive research has focused on engineering artificial SEI layers to enhance the stability and longevity of lithium metal electrodes. Various approaches have been explored, including artificial solid–electrolyte interphases (ASEIs), modifications to the electrolyte, and nanostructured electrode architectures.[21–23] Among these, the incorporation of advanced coating materials has shown significant promise in mitigating dendrite growth and enhancing SEI stability. In particular, silicon nitride (Si_3N_4) has emerged as a promising candidate due to its exceptional thermal stability, high mechanical strength, and ability to form lithium nitride (Li_3N) during the pretreatment.[24] The presence of nitride-rich layers has been shown to enhance the mechanical stability of the SEI while simultaneously facilitating lithium-ion transport, thereby improving overall cycling stability.[25]

In this study, we explore the role of nano-Si_3N_4 as an additive in the formation of artificial SEI to enhance the stability and performance of lithium metal electrodes. By evaluating the electrochemical behavior, cycling stability, and morphology evolution of Si_3N_4-treated lithium metal electrodes, we aim to provide insights into the development of more durable and safer lithium metal batteries. The findings from this study will

[a]*Department of Mechanical Engineering, Catholic University of America, Washington, DC, 20064, USA. E-mail: linc@cua.edu*

[b]*Department of Chemistry, Catholic University of America, Washington, DC, 20064, USA*

† These authors contributed equally to the work.

contribute to the ongoing efforts to address the challenges associated with lithium metal anodes, paving the way for their broader adoption in next-generation high-energy-density battery technologies.

2 Experimental section

2.1 Materials and preparation

Lithium metal (99.9%, Thermo Fisher Scientific) was manually rolled to achieve a glossy surface and subsequently punched into $\frac{1}{2}$-inch diameter disks. These disks were placed onto 0.5 mm-thick stainless-steel substrates. Nano-sized silicon nitride (Si_3N_4) powder (<50 nm, spherical), dimethyl carbonate (DMC), ethylene carbonate (EC), and 1 M lithium hexafluorophosphate ($LiPF_6$) in a 50 : 50 EC : DEC (ethylene carbonate : diethyl carbonate) solution were obtained from Sigma-Aldrich.

The detailed procedure for sample preparation, along with the corresponding schematic shown in Fig. 1, will be presented in the Results and discussion section.

2.2 Materials characterization

The surface morphology of untreated and treated lithium, both before and after cycling, was determined using scanning electron microscopy (SEM) and X-ray diffraction (XRD). SEM imaging was conducted with a Hitachi SU-70 FEG, and XRD measurements were performed using a Rigaku SmartLab XRD.

2.3 Electrochemical characterization

CR2032 coin-type symmetric cells were assembled in an argon-filled glove box. Each cell contained 80 μL of 1 M $LiPF_6$ dissolved in a 1 : 1 mixture of ethylene carbonate (EC) and diethyl carbonate (DEC) as the electrolyte. Two layers of 5/8-inch Celgard 2400 separators were used to isolate the electrodes. Electrochemical impedance spectroscopy (EIS) measurements were performed using a Gamry Interface 1010E. The frequency range spanned from 1 MHz to 100 mHz, with an applied AC voltage amplitude of 10 mV. Cyclability was evaluated by a Neware battery testing system (BTS8.0), where a current of ±1 mA cm^{-2} applied for one-hour intervals, alternating between charge and discharge.

3 Result and discussion

Fig. 1a and b illustrates the detailed procedure utilized for preparing silicon nitride (Si_3N_4)-based artificial solid electrolyte interphase (ASEI) layers on lithium metal surfaces. Silicon nitride nanoparticles (<50 nm, spherical morphology) were chosen for their high surface area, which promotes excellent dispersion in solvents and facilitates the formation of uniform, compact protective layers. A study by Damircheli *et al.* confirmed that the Si_3N_4 nanoparticle structure tends to yield more uniform and mechanically robust coatings compared to micro-sized silicon nitride, which is essential for effectively

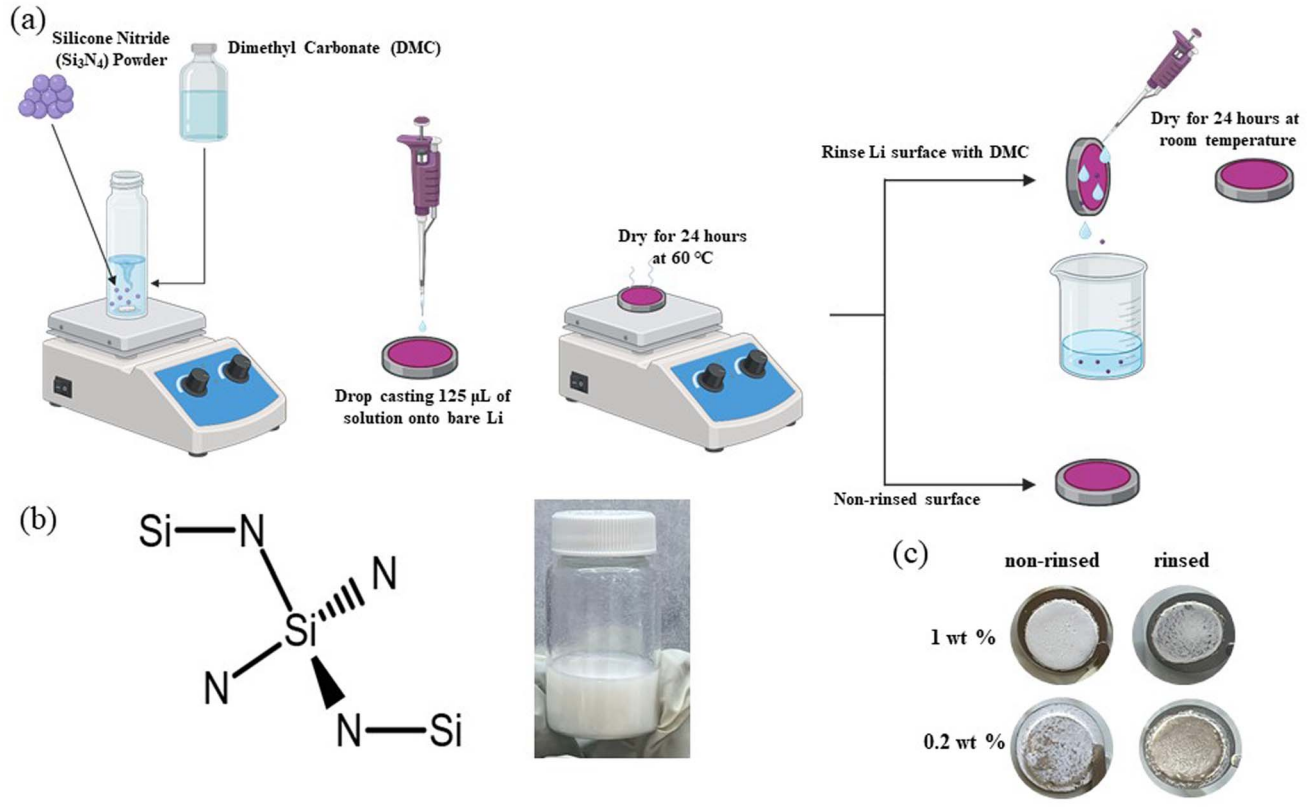

Fig. 1 (a) Schematic illustration showing the formation of the artificial nano Si_3N_4 layer on lithium metal. (b) Structural representation of Si_3N_4 and 1 wt% nano Si_3N_4 dispersed in DMC. (c) Comparative analysis of 1 wt% and 0.2 wt% samples, including rinsed and non-rinsed conditions.

mitigating dendrite growth and enhancing overall sodium metal battery performance.[25]

Two distinct concentrations, 0.2 wt% and 1 wt%, of Si_3N_4 nanoparticles were dispersed in dimethyl carbonate (DMC), as illustrated in Fig. 1b. DMC was selected as a solvent due to its good compatibility with lithium metal and its suitable volatility, ensuring reasonable evaporation upon drying without leaving significant residues. The nanoparticle solutions underwent continuous stirring for 24 hours at room temperature. This extended stirring period was critical to disrupt nanoparticle agglomerations, ensuring homogeneous dispersion and preventing particle settling, thereby guaranteeing consistency in the subsequent coating process.

Precisely 125 μL of the homogenized Si_3N_4/DMC suspension was drop-cast onto pristine lithium metal disks, which had been previously rolled and punched to standardize dimensions and ensure surface uniformity. The coated lithium disks were then carefully dried at a controlled temperature of 60 °C for 24 hours. This moderate drying condition allowed for thorough evaporation of the DMC solvent without causing thermal degradation or morphological alteration of either the nanoparticles or the lithium metal substrate.

To investigate the impact of the coverage of the ASEI layer on its performance, a subset of coated samples underwent an additional rinsing step. This involved gently rinsing the dried lithium surfaces with pure DMC, removing loosely adhered or excessive nanoparticles. Conversely, non-rinsed samples were prepared to retain the complete deposited quantity of Si_3N_4 nanoparticles, allowing comparative analysis of the coating coverage and its subsequent performance, as shown in Fig. 1a.

The comparative photographic images in Fig. 1c highlight visible differences between rinsed and non-rinsed samples at both concentrations (0.2 wt% and 1 wt%), clearly illustrating variations in particle distribution and surface coverage. These observations underscore the significance of both nanoparticle concentration and the rinsing process in determining the final characteristics of the ASEI layer.

Fig. 2 presents comprehensive characterization results of Si_3N_4-based artificial solid electrolyte interphase (ASEI) layers prepared on lithium metal substrates, highlighting morphological and compositional differences under varying sample conditions. Top-view scanning electron microscopy (SEM) images shown in Fig. 2a–d offer detailed insights into the surface morphologies of rinsed and non-rinsed 1 wt% Si_3N_4/Li samples. The SEM analysis differentiates between the two preparation conditions. The rinsed samples exhibit relatively dispersed Si_3N_4 nanoparticles with intermittent agglomeration, indicative of partial nanoparticle detachment or redistribution due to the rinsing step. Conversely, the non-rinsed samples demonstrate a noticeably thick and interconnected structure, signifying the presence of a denser nanoparticle distribution and a thicker ASEI layer. The thickness of this layer is approximately 20 μm, as shown in Fig. S3. Such a thick layer with interconnectivity potentially influences ionic transport pathways and mechanical properties of the ASEI layers.

The structural and compositional analysis through X-ray diffraction (XRD), presented in Fig. 2e, provides further clarity on the chemical interactions and resultant products formed during the ASEI formation process. The XRD pattern of the nano Si_3N_4 powder used in this work is shown in Fig. S1, and the XRD profile of the stainless-steel substrate is provided in Fig. S2. Prominent diffraction peaks at 51.9° in both 1 wt% and 0.2 wt% non-rinsed samples are attributed to lithium nitride (Li_3N), indicating the effective chemical reaction between lithium metal and Si_3N_4 nanoparticles according to eqn (1):

$$Si_3N_4 + 12\ Li \rightarrow 4\ Li_3N + 3\ Si \quad (1)$$

Additionally, the persistence of a weaker diffraction peak at approximately 32.5°, representative of residual Si_3N_4, highlights incomplete consumption of the nanoparticles, even post-rinsing. This confirms nanoparticle retention and provides evidence of their sustained presence on the lithium surface. A notable distinction arises at the diffraction peak around 36.1°, attributed to metallic lithium. This peak shows significantly greater intensity in the 0.2 wt% Si_3N_4 sample compared to the 1 wt% sample, reflecting differences in nanoparticle-lithium interaction dynamics. Specifically, the higher nanoparticle concentration in the 1 wt% samples promotes extensive lithium consumption through reaction, subsequently reducing the intensity of the metallic lithium peak.[26–30]

The comparative analysis of XRD and SEM data underscores the critical influence of nanoparticle concentration on the ASEI layer properties. Higher nano Si_3N_4 concentrations not only enhance the density and uniformity of the formed ASEI but also significantly modify the lithium-metal surface chemistry through more pronounced reactions. These detailed observations elucidate the intricate balance required in optimizing nanoparticle concentration and processing steps to achieve high-quality, uniform, and effective ASEI layers essential for advanced lithium-metal battery applications.

Fig. 3 illustrates galvanostatic cycling profiles comparing the electrochemical stability and performance longevity of lithium-metal symmetric cells under varying Si_3N_4 nanoparticle treatments. These tests were conducted at a constant current density of 1 mA cm^{-2} and a fixed capacity of 1 mAh cm^{-2} using an electrolyte consisting of 1 M $LiPF_6$ dissolved in EC : DEC (1 : 1 volume ratio). The voltage-time behavior of bare lithium electrodes, alongside lithium electrodes treated with 0.2 wt% and 1.0 wt% Si_3N_4 nanoparticles under rinsed and non-rinsed conditions, is analyzed systematically.

The bare lithium electrode exhibited rapid deterioration (Fig. 3a), characterized by escalating voltage instability and eventual short-circuit behavior within approximately 280 hours, marking the inherent instability of pristine lithium surfaces under repetitive plating and stripping cycles. Conversely, lithium electrodes treated with 0.2 wt% Si_3N_4 displayed notable improvements in cycling stability, with rinsed and non-rinsed samples demonstrating stable cycling up to approximately 550 hours and 425 hours, respectively. However, subsequent voltage fluctuations indicated gradual SEI instability, presumably due to poor nano-Si_3N_4 coverage and inconsistent ASEI layer formation that left localized lithium surface areas exposed. This non-uniform ASEI layer facilitates uneven Li-ion plating and

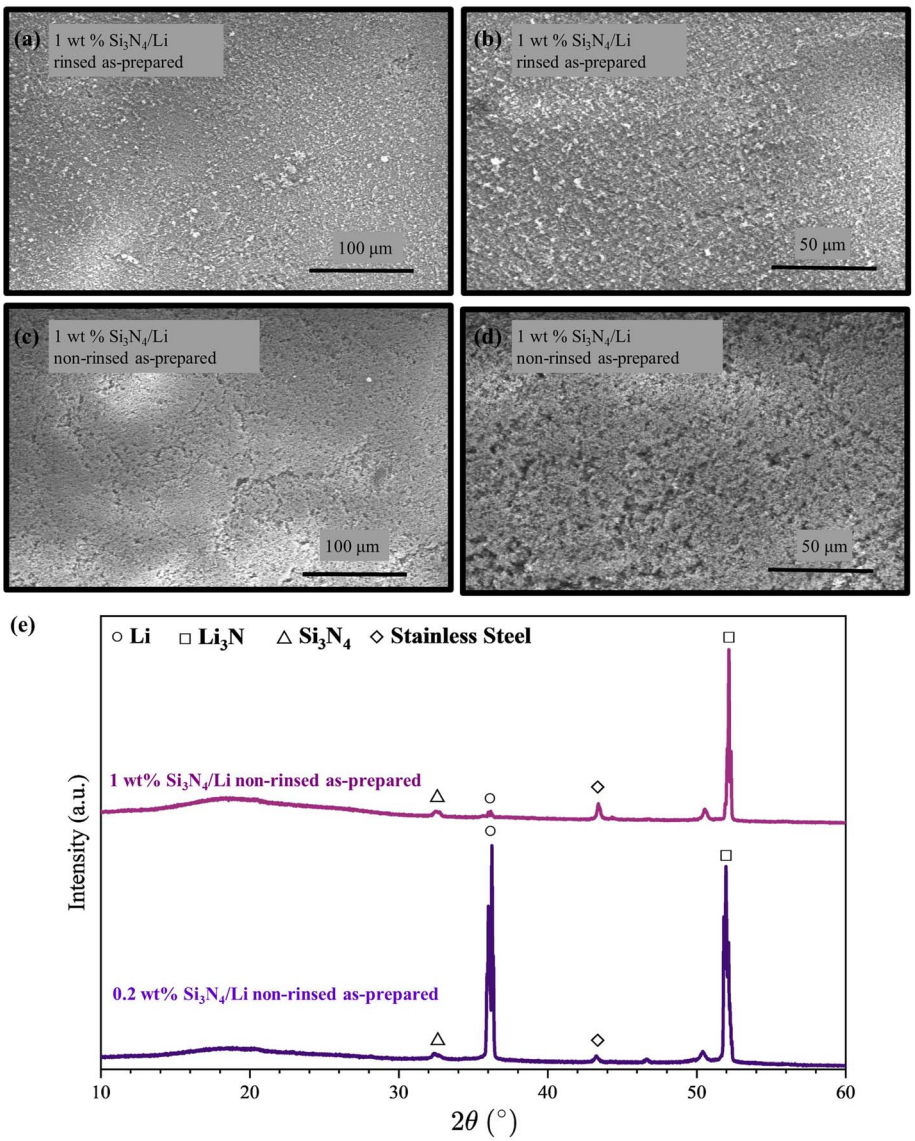

Fig. 2 (a–d) Top-view SEM images of 1 wt% nano Si_3N_4/Li samples, rinsed and non-rinsed samples in their as-prepared state. (e) XRD patterns of 1 wt% and 0.2 wt% nano Si_3N_4/Li non-rinsed as-prepared samples on a stainless-steel substrate.

stripping processes that result in dendrite formation eventually, causing internal short circuits that abruptly terminate cell functionality.

Remarkably, the rinsed 1.0 wt% Si_3N_4-treated lithium cell, as shown in Fig. 3a, demonstrated substantial stability improvements, maintaining stable voltage profiles up to approximately 950 hours before exhibiting similar voltage instabilities to the lower concentration samples. This observation underscores the effectiveness of a denser nano-Si_3N_4 particle-induced ASEI, even after partial removal *via* rinsing, in prolonging electrode stability by uniformly covering more of the lithium surface and effectively suppressing dendrite initiation.

The most significant enhancement in electrochemical stability is observed in the non-rinsed 1.0 wt% nano-Si_3N_4-treated lithium electrode (Fig. 3b), which sustained stable cycling conditions for nearly 1375 hours, approximately fivefold longer than the bare lithium sample. After about 1000 hours, a gradual increase in voltage hysteresis emerged, indicative of incremental SEI thickening over prolonged cycling. Importantly, this thickening occurs at a significantly mitigated rate compared to untreated lithium, suggesting robust, ion-permeable properties attributed to the intact, continuous ASEI layer formed by higher Si_3N concentrations without rinsing. This result correlates with previous morphological analyses (Fig. 2), demonstrating a good ASEI uniformity and integrity in non-rinsed condition, such enhancements underscore the role of strategically engineered nanoparticle treatments to advance long-term stability and reliability in lithium-based energy storage systems.

Fig. 4 provides post-mortem analyses of Li metal anodes to reveal its morphological, structural, and chemical evolution of lithium-metal anodes treated with 1 wt% Si_3N_4 nanoparticles,

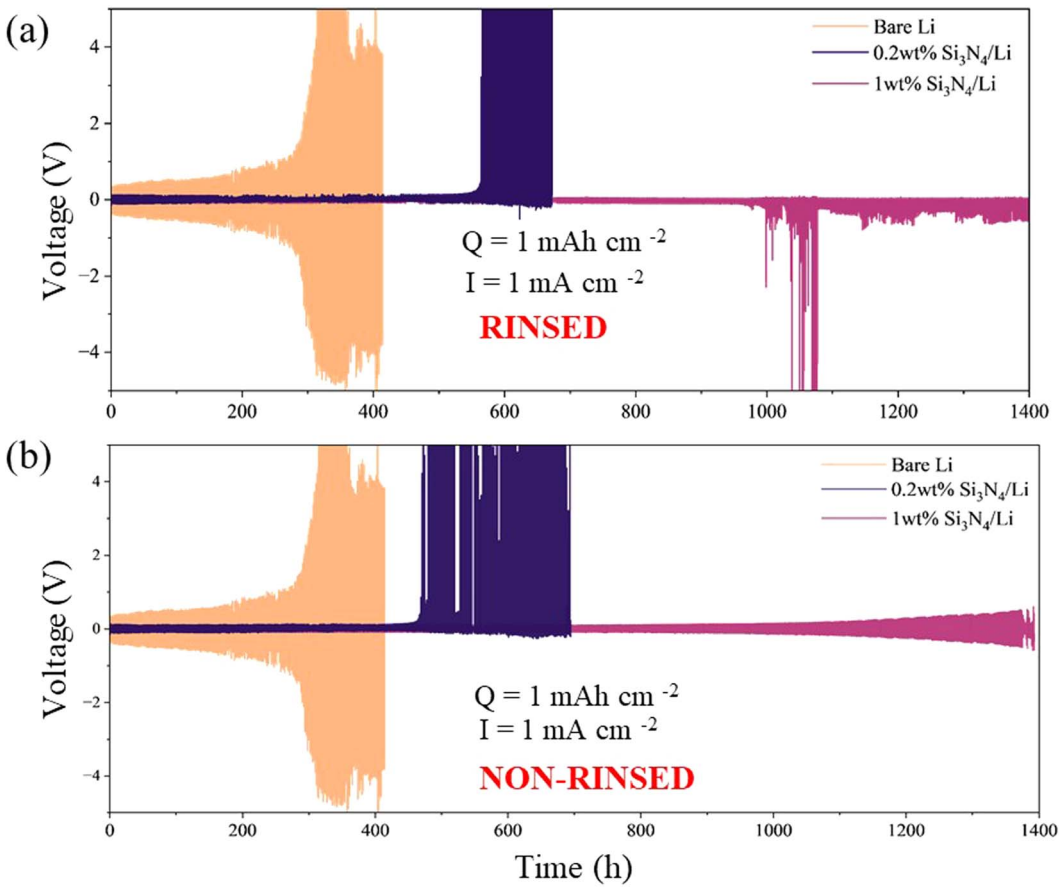

Fig. 3 Cycling performance of symmetric Li/x% Si_3N_4 (x = 1 and 0.2 wt%) (a) rinsed and (b) non-rinsed.

assessing their interfacial stability throughout cycling. Fig. 4a and b shows top-view SEM images of 1 wt% Si_3N_4/Li samples in non-rinsed conditions after 400 hours of cycling, revealing a uniform surface morphology with no trace of 3D dendritic structures, which indicates the presentence of the dendrites (schematic illustration in Fig. 4e). In contrast, bare lithium after 300 hours of cycling exhibits obvious 3D structures characteristic of dendrite formation, as shown in Fig. S4. This indicates the effectiveness of Si_3N_4 nanoparticles in forming a stable and robust SEI layer capable of withstanding mechanical stresses and volume fluctuations during prolonged lithium cycling.

Fig. 4c and d exhibits Nyquist plots, from electrochemical impedance spectroscopy (EIS), of bare lithium and Si_3N_4-treated lithium electrodes at selected intervals (1st, 50th, 100th, 150th, and 200th cycles). High-frequency semicircles, indicative of charge-transfer resistance at the electrode–electrolyte interface, offer insights into the dynamic evolution of SEI layers under repetitive cycling. Electrochemical impedance spectra for bare Li and 1 wt% Li/nano-Si_3N_4 electrodes, along with their fitted curves and corresponding equivalent circuits, are provided in Fig. S5 (SI). In these plots, the colored square symbols represent the measured impedance data, and the black lines show the corresponding fitting results. The equivalent circuit diagrams included in the figures illustrate the model used for fitting, which effectively captures the interfacial and charge-transfer processes observed in the measurements.

Initially, both the bare and treated lithium electrodes demonstrate comparable impedance behaviors, characterized by relatively high charge-transfer resistances (~90 Ω), consistent with typical early-cycle phenomena involving surface heterogeneity and evolving SEI formation. During subsequent cycling, a gradual decrease in impedance occurs due to stabilization and structural refinement of the SEI layer. However, after approximately 200 cycles, the bare lithium electrode reveals a notable impedance increase, suggesting instability and accelerated SEI degradation. This elevated impedance is symptomatic of growing SEI thickness, formation of insulating decomposition products, and diminished interfacial ionic conductivity, contributing to reduced battery efficiency and eventual cell failure.

Conversely, the 1 wt% nano Si_3N_4-treated lithium electrodes display remarkable impedance stability even after extensive cycling, signifying a robust and conductive SEI formation. This stable impedance profile highlights the pivotal role of Si_3N_4 nanoparticles, along with the formation of Li_3N interlayer, in fostering a chemically uniform and mechanically resilient interfacial layer that effectively mitigates impedance escalation typically associated with prolonged lithium cycling. Such

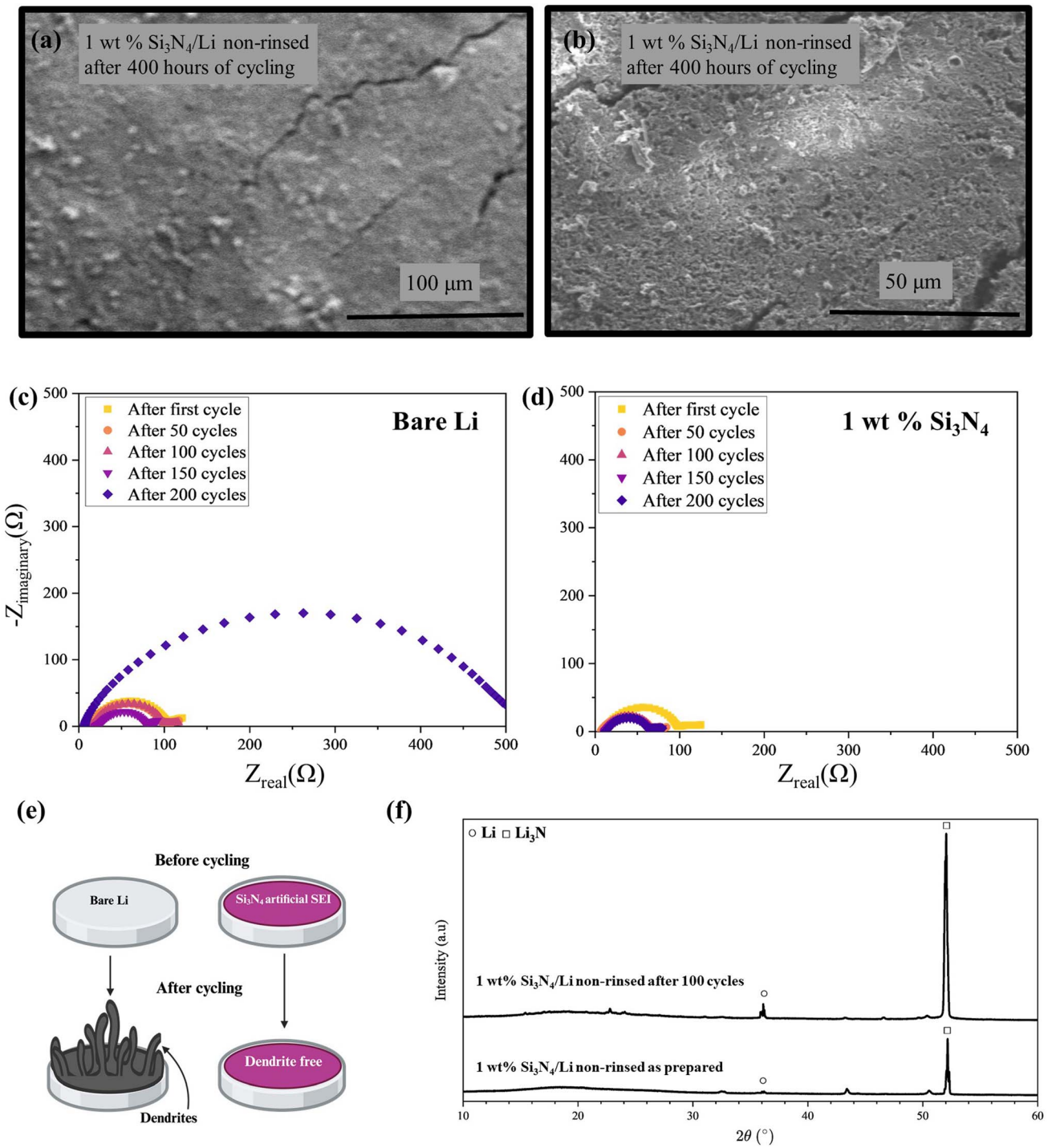

Fig. 4 (a and b) Top-view SEM images of 1 wt% nano Si_3N_4/Li samples, non-rinsed, after 400 hours of cycling. (c and d) Electrochemical impedance of bare Li and 1 wt% Li/nano Si_3N_4 after x ($x = 1$, 50, 100, 50, 200 cycles). (e) Dendrite growth schematic (f) XRD patterns of 1 wt% Li/nano Si_3N_4 non-rinsed as prepared and after 100 cycles samples on a stainless-steel substrate.

behavior is essential for enhancing ion transport dynamics, preserving interface integrity, and extending battery cycle life.

X-ray diffraction (XRD) analyses depicted in Fig. 4f further elucidate the chemical transformations occurring during cycling. Initially, the as-prepared 1 wt% Si_3N_4 non-rinsed lithium electrode presents minimal Li_3N formation, as indicated by a low-intensity diffraction peak at 51.9°.[31–34] However, post-100 cycles, the significant amplification of this peak intensity indicates enhanced Li_3N formation. This phenomenon underscores the progressive reaction between lithium and Si_3N_4 nanoparticles, fostering a chemically enriched Li_3N-dominated SEI that exhibits superior ionic

conductivity and mechanical strength. Li_3N's presence is instrumental in improving electrochemical stability by providing a durable and conductive interface, significantly reducing charge transfer resistance, and effectively hindering dendrite nucleation.

Collectively, these findings provide compelling evidence that incorporating Si_3N_4 nanoparticles significantly enhances lithium-metal electrode stability, emphasizing the critical interplay between SEI chemical composition, mechanical resilience, and electrochemical performance. These insights offer a strategic approach for improving long-term stability and reliability in advanced lithium-metal battery technologies.

4 Conclusion

In conclusion, this study systematically explores the incorporation of nano-sized silicon nitride (Si_3N_4) additives in lithium-metal batteries, demonstrating substantial improvements in anode stability and electrochemical performance. Through detailed morphological, structural, and electrochemical analyses, it was demonstrated that Si_3N_4 nanoparticles significantly facilitate the formation of a robust and Li_3N-rich artificial solid electrolyte interphase (ASEI). This specialized ASEI effectively mitigates dendrite formation and propagation, markedly enhancing both the mechanical resilience and ionic conductivity of the lithium-metal interface.

Comparative assessments between rinsed and non-rinsed treatment methodologies underscored the crucial role of the uniform surface coverage of the nanoparticle on the lithium surface. The non-rinsed 1 wt% Si_3N_4-treated lithium electrodes showcased notably superior cycling stability, sustaining stable electrochemical performance for up to 1375 hours, a significant improvement over the rinsed counterpart's 950-hour lifespan. Such findings emphasize the strategic advantage of maintaining the nanoparticle additive layer intact, highlighting its critical function in stabilizing lithium metal surfaces and extending operational longevity.

Overall, this research highlights nano-silicon nitride as an effective and promising additive for overcoming key challenges associated with lithium-metal anodes, including dendrite suppression and solid electrolyte interphase stabilization. These advancements are instrumental in promoting the broader application and reliability of high-energy-density lithium-metal battery systems, significantly contributing to their potential usage in electric vehicles, portable electronic devices, and large-scale energy storage solutions.

Conflicts of interest

There are no conflicts to declare.

Data availability

The data supporting the findings of this study are comprehensively detailed within the main manuscript, which includes all critical figures, and experimental results such as high-resolution SEM images, XRD spectra, Nyquist plots, and cyclic deposition/stripping performance data. Due to confidentiality and intellectual property considerations, certain raw data, including proprietary synthesis protocols and specific experimental details, cannot be publicly disclosed. However, the processed data, which have been rigorously analyzed and are essential for reproducing the findings of this study, are available upon reasonable request. Interested researchers should contact the corresponding author, Dr Chuan-fu Lin, to discuss data access and any necessary agreements to ensure appropriate use and protection of the information.

Additional supporting data, are available in the SI accompanying this article. See DOI: **https://doi.org/10.1039/d5ra05077d**.

Acknowledgements

This work was supported by the U.S. Department of Energy, Office of Science, Office of Basic Energy Sciences, under award number DE-SC0024274. The authors would like to thank Dr Konstantin Gilbo, from the Vitreous State Laboratory, for his assistance with the XRD analysis.

References

1 T. Kim, W. Song, D.-Y. Son, L. K. Ono and Y. Qi, Lithium-Ion Batteries: Outlook on Present, Future, and Hybridized Technologies, *J. Mater. Chem. A*, 2019, **7**(7), 2942–2964, DOI: **10.1039/C8TA10513H**.

2 M. Li, J. Lu, Z. Chen and K. Amine, 30 Years of Lithium-Ion Batteries, *Adv. Mater.*, 2018, **30**(33), 1800561, DOI: **10.1002/adma.201800561**.

3 A. E. Gerdroodbar, H. Alihemmati, S.-A. Safavi-Mirmahaleh, M. Golshan, R. Damircheli, S. N. Eliseeva and M. Salami-Kalajahi, A Review on Ion Transport Pathways and Coordination Chemistry between Ions and Electrolytes in Energy Storage Devices, *J. Energy Storage*, 2023, **74**, 109311, DOI: **10.1016/j.est.2023.109311**.

4 A. Ourang, S. Pilehvar, M. Mortezaei and R. Damircheli, Effect of Aluminum Doped Iron Oxide Nanoparticles on Magnetic Properties of the Polyacrylonitrile Nanofibers, *J. Polym. Eng.*, 2017, **37**(2), 135–141, DOI: **10.1515/polyeng-2015-0303**.

5 B. Scrosati, J. Hassoun and Y.-K. Sun, Lithium-Ion Batteries. A Look into the Future, *Energy Environ. Sci.*, 2011, **4**(9), 3287, DOI: **10.1039/c1ee01388b**.

6 G. E. Blomgren, The Development and Future of Lithium Ion Batteries, *J. Electrochem. Soc.*, 2017, **164**(1), A5019–A5025, DOI: **10.1149/2.0251701jes**.

7 B. R. Pant, Y. Ren and Y. Cao, Dendrite Growth and Dead Lithium Formation in Lithium Metal Batteries and Mitigation Using a Protective Layer: A Phase-Field Study, *ACS Appl. Mater. Interfaces*, 2024, **16**(42), 56947–56956, DOI: **10.1021/acsami.4c08605**.

8 A. Enayati Gerdroodbar, R. Damircheli, S. N. Eliseeva and M. Salami-Kalajahi, Janus Structures in Energy Storage Systems: Advantages and Challenges, *J. Electroanal. Chem.*, 2023, **948**, 117831, DOI: **10.1016/j.jelechem.2023.117831**.

9 J. Li, Z. Kong, X. Liu, B. Zheng, Q. H. Fan, E. Garratt, T. Schuelke, K. Wang, H. Xu and H. Jin, Strategies to Anode Protection in Lithium Metal Battery: A Review, *InfoMat*, 2021, **3**(12), 1333–1363, DOI: **10.1002/inf2.12189**.

10 L.-P. Hou, X.-Q. Zhang, B.-Q. Li and Q. Zhang, Challenges and Promises of Lithium Metal Anode by Soluble Polysulfides in Practical Lithium–Sulfur Batteries, *Mater. Today*, 2021, **45**, 62–76, DOI: **10.1016/j.mattod.2020.10.021**.

11 S. Li, M. Jiang, Y. Xie, H. Xu, J. Jia and J. Li, Developing High-Performance Lithium Metal Anode in Liquid Electrolytes: Challenges and Progress, *Adv. Mater.*, 2018, **30**(17), 1800561, DOI: **10.1002/adma.201706375**.

12 J. Wang, B. Ge, H. Li, M. Yang, J. Wang, D. Liu, C. Fernandez, X. Chen and Q. Peng, Challenges and Progresses of Lithium-Metal Batteries, *Chem. Eng. J.*, 2021, **420**, 129739, DOI: **10.1016/j.cej.2021.129739**.

13 A. Varzi, R. Raccichini, S. Passerini and B. Scrosati, Challenges and Prospects of the Role of Solid Electrolytes in the Revitalization of Lithium Metal Batteries, *J. Mater. Chem. A*, 2016, **4**(44), 17251–17259, DOI: **10.1039/C6TA07384K**.

14 J. R. Nair, L. Imholt, G. Brunklaus and M. Winter, Lithium Metal Polymer Electrolyte Batteries: Opportunities and Challenges, *Electrochem. Soc. Interface*, 2019, **28**(2), 55–61, DOI: **10.1149/2.F05192if**.

15 K. B. Hatzell, X. C. Chen, C. L. Cobb, N. P. Dasgupta, M. B. Dixit, L. E. Marbella, M. T. McDowell, P. P. Mukherjee, A. Verma, V. Viswanathan, A. S. Westover and W. G. Zeier, Challenges in Lithium Metal Anodes for Solid-State Batteries, *ACS Energy Lett.*, 2020, **5**(3), 922–934, DOI: **10.1021/acsenergylett.9b02668**.

16 R. Damircheli, B. Hoang, V. Castagna Ferrari and C.-F. Lin, Fluorinated Artificial Solid–Electrolyte–Interphase Layer for Long-Life Sodium Metal Batteries, *ACS Appl. Mater. Interfaces*, 2023, **15**(47), 54915–54922, DOI: **10.1021/acsami.3c12351**.

17 A. Mauger, M. Armand, C. M. Julien and K. Zaghib, Challenges and Issues Facing Lithium Metal for Solid-State Rechargeable Batteries, *J. Power Sources*, 2017, **353**, 333–342, DOI: **10.1016/j.jpowsour.2017.04.018**.

18 Y. Chen, Y. Luo, H. Zhang, C. Qu, H. Zhang and X. Li, The Challenge of Lithium Metal Anodes for Practical Applications, *Small Methods*, 2019, **3**(7), 1800551, DOI: **10.1002/smtd.201800551**.

19 C. Heubner, S. Maletti, H. Auer, J. Hüttl, K. Voigt, O. Lohrberg, K. Nikolowski, M. Partsch and A. Michaelis, From Lithium-Metal toward Anode-Free Solid-State Batteries: Current Developments, Issues, and Challenges, *Adv. Funct. Mater.*, 2021, **31**(51), 2106608, DOI: **10.1002/adfm.202106608**.

20 V. Raj, N. P. B. Aetukuri and J. Nanda, Solid State Lithium Metal Batteries – Issues and Challenges at the Lithium-Solid Electrolyte Interface, *Curr. Opin. Solid State Mater. Sci.*, 2022, **26**(4), 100999, DOI: **10.1016/j.cossms.2022.100999**.

21 Y. E. Park, M. K. Oh, H. T. Sim, H. J. Kim, Y. S. Cho, S. J. Park and D. W. Kim, Rationally Designed Li-Ag Alloy with In-Situ-Formed Solid Electrolyte Interphase for All-Solid-State Lithium Batteries, *ACS Appl. Mater. Interfaces*, 2024, **16**(30), 39460–39469, DOI: **10.1021/acsami.4c08541**.

22 Y. Luo, X. Liu, P. Li, W. Zhang, H. Ding, M. Li and Z. Rao, N-Rich Bilayer Solid Electrolyte Interphase toward Highly Reversible Lithium Metal Batteries, *ACS Appl. Mater. Interfaces*, 2024, **16**(10), 12479–12485, DOI: **10.1021/acsami.3c18071**.

23 Q. Chen, M. Mo, N. Chen, T. Gao, R. Lang, Z. Tan, J. Xing and J. Zhu, Simultaneous Improvement of Energy Storage Characteristics and Temperature Stability in K0.5Na0.5NbO3-Based Ceramics via LiF Modification, *ACS Appl. Mater. Interfaces*, 2024, **16**(39), 52487–52500, DOI: **10.1021/acsami.4c11906**.

24 Z. Krstic and V. D. Krstic, Silicon Nitride: The Engineering Material of the Future, *J. Mater. Sci.*, 2012, 535–552, DOI: **10.1007/s10853-011-5942-5**.

25 R. Damircheli, B. Hoang, V. C. Ferrari and C. F. Lin, Highly Uniform Nitride-Rich Artificial Solid Electrolyte Interphase Enabled by Nano-Silicon Nitride for Superior Performance in Advanced Sodium Metal Batteries, *J. Mater. Chem. A*, 2024, **12**(46), 31949–31958, DOI: **10.1039/d4ta05595k**.

26 M. Yang, K. Yang, Y. Wu, Z. Wang, T. Ma, D. Wu, L. Yang, J. Xu, P. Lu, J. Peng, Z. Jiang, X. Zhu, Q. Gao, F. Xu, L. Chen, H. Li and F. Wu, Dendrite-Free All-Solid-State Lithium Metal Batteries by In Situ Phase Transformation of the Soft Carbon–Li $_3$ N Interface Layer, *ACS Nano*, 2024, **18**(26), 16842–16852, DOI: **10.1021/acsnano.4c02509**.

27 X. Xu, G. Du, C. Cui, J. Liang, C. Zeng, S. Wang, Y. Ma and H. Li, Stabilizing the Halide Solid Electrolyte to Lithium by a β-Li $_3$ N Interfacial Layer, *ACS Appl. Mater. Interfaces*, 2022, **14**(35), 39951–39958, DOI: **10.1021/acsami.2c09131**.

28 Y.-S. Chen, J.-K. Chang and Y.-S. Su, Engineering a Lithium Silicate-Based Artificial Solid Electrolyte Interphase for Enhanced Rechargeable Lithium Metal Batteries, *Surf. Coat. Technol.*, 2024, **480**, 130617, DOI: **10.1016/j.surfcoat.2024.130617**.

29 M. Wu, Z. Wen, Y. Liu, X. Wang and L. Huang, Electrochemical Behaviors of a Li3N Modified Li Metal Electrode in Secondary Lithium Batteries, *J. Power Sources*, 2011, **196**(19), 8091–8097, DOI: **10.1016/j.jpowsour.2011.05.035**.

30 H. Xu, Y. Li, A. Zhou, N. Wu, S. Xin, Z. Li and J. B. Goodenough, Li $_3$ N-Modified Garnet Electrolyte for All-Solid-State Lithium Metal Batteries Operated at 40 °C, *Nano Lett.*, 2018, **18**(11), 7414–7418, DOI: **10.1021/acs.nanolett.8b03902**.

31 A. Kızılaslan and H. Akbulut, Assembling All-Solid-State Lithium–Sulfur Batteries with Li $_3$ N-Protected Anodes, *Chempluschem*, 2019, **84**(2), 183–189, DOI: **10.1002/cplu.201800539**.

32 C. Liu, T. Li, H. Zhang, Z. Song, C. Qu, G. Hou, H. Zhang, C. Ni and X. Li, DMF Stabilized Li3N Slurry for Manufacturing Self-Prelithiatable Lithium-Ion Capacitors, *Sci. Bull.*, 2020, **65**(6), 434–442, DOI: **10.1016/j.scib.2019.11.014**.

33 C. B. Minella, C. Rongeat, R. Domènech-Ferrer, I. Lindemann, L. Dunsch, N. Sorbie, D. H. Gregory and O. Gutfleisch, Synthesis of LiNH2 + LiH by Reactive Milling of Li3N, *Faraday Discuss.*, 2011, **151**, 253, DOI: **10.1039/c1fd00009h**.

34 T. Furukawa, Y. Hirakawa, H. Kondo and T. Kanemura, Dissolution Behavior of Lithium Compounds in Ethanol, *Nucl. Mater. Energy*, 2016, **9**, 286–291, DOI: **10.1016/j.nme.2016.05.005**.